國立臺灣大學醫學院分子醫學研究所

碩士論文

Graduate Institute of Molecular Medicine

College of Medicine

National Taiwan University

Master Thesis

Rab11 在果蠅感覺神經元之研究

The role of Rab11 in *Drosophila* sensory neurons

周芝妤

Chih-Yu Chou

指導教授：李秀香 博士

Advisor: Hsiu-Hsiang Lee, Ph.D.

中華民國 106 年 7 月

July 2017

中文摘要

　　當果蠅經歷完全變態的過程中，果蠅感覺神經元的樹突修剪作用是一個必要的過程。樹突修剪作用受到嚴格的調控，任何錯誤調控可能會對神經系統帶來嚴重後果。樹突修剪的詳細機制仍然不清楚。我們發現，Rab11 這個小 G 蛋白會參與果蠅感覺神經元的樹突修剪。為了闡明 Rab11 的 GTP 酶對於樹突修剪的重要性，我們利用針對 GTP 酶活性的兩個突變(constitutively active 和 dominant negative 突變)，證明 GTP 酶的活性對果蠅感覺神經元的樹突修剪是重要的。Rab11 蛋白被發現在果蠅 S2 細胞中，以及感覺神經元之中會和捲曲螺旋蛋白 Spindle-F (Spn-F)有交互作用。本實驗室先前研究發現，在果蠅感覺神經元的樹突修剪之中，Spn-F 會調控 Ik2 蛋白激酶的訊號傳遞。我們更進一步發現在 Spn-F 蛋白 C-terminus 的區域中有一蛋白質結構域對 SpnF 和 Rab11 交互作用是重要的。最後，我們在螢光共軛焦顯微鏡下觀察到在近神經元本體的樹突上 Rab11 小泡的移動，而且我們也藉由在神經中大量表現突變的 Rab11，觀察到在樹突修剪中，被切斷的樹突位置附近，Rab11 的活化對樹突 varicosity 的形成是必要的。
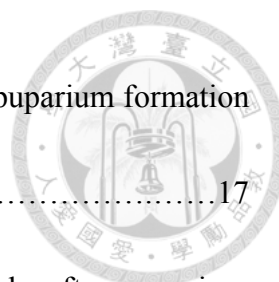
Abstract

During metamorphosis, there is an essential process in *Drosophila* Class IV dendritic arborization (C4da) sensory neurons called dendrite pruning. Pruning is a tightly controlled process and any mis-regulation could bring serious consequences to the nervous system. The detailed mechanism of pruning is still remains unclear. We identify a small G protein Rab11 which is involved in the dendrite pruning of Drosophila class IV da neuron. To examine whether the GTPase activity of Rab11 is required for dendrite pruning, we generated constitutively active (CA) and dominant negative (DN) form of Rab11. We found that overexpression of CA-Rab11 in class IV da neurons does not affect dendrite pruning, but overexpression of DN-Rab11 impaired dendrite pruning, suggesting the GTPase activity of Rab11 is critical for dendrite pruning of class IV da neuron. Rab11 was detected in complexes with Spindle-F (Spn-F), which mediates Ik2 kinase signaling in class IV da neurons during pruning, not only in S2 cells, but also in neurons. We further identified a region at C-terminus of Spn-F protein that is important for Spn-F to associate with Rab11 in S2 cells. Finally, we characterized the movement of Rab11 vesicles in the proximal dendrites, and found that wild-type and CA-Rab11, but not DN-Rab11, could be observed in varicosities, which occur around the dendrite severing sites during early pruning.

CONTENTS

List of Figures

List of Tables

Introduction

1. Neuron pruning

Neuron pruning is a remodeling process of neurons to eliminate certain neurites or synapses to ensure the correct connection of nervous system. Pruning occurs in different species and cell types, for example: mammalian cerebellar granule neurons, Xenopus optic tectal neurons, *C. elegans*, *Drosophila* mushroom bodies and dendritic arborization (da) neurons (Puram, S. V. and Bonni, A., 2013). In vertebrate nervous system, it has been demonstrated that several mechanisms are used to ensure the correct connections, and often related to plasticity of developmental brain (Luo and O'Leary, 2005). The critical steps of pruning were well defined, but the underlying mechanisms remain unclear.

2. Our model for dendrite pruning: Drosophila class IV dendritic arborization (da) neurons

In *Drosophila*, some neurons prune their larval axons and/or dendrites during metamorphosis (Schubiger et al., 1998, Truman, 1990). In the central nervous system (CNS) of *Drosophila*, the γ neurons of mushroom body (MB) prune their branches of dorsal/medial axon through glia-mediated engulfment and local degeneration (Awasaki

1

and Ito, 2004). In the peripheral nervous system (PNS), some of the dorsal group of da neurons, such us class I ddaD/E neurons and class IV ddaC neurons, only eliminate their larval dendrites first and regrow the adult-specific dendrites at later stages, but their axons remain intact (Williams and Truman, 2005). The events of dendrite pruning of class IV da neurons are well-defined; therefore, it is a good model to study the molecular mechanisms of dendrite pruning. The dendrites of class IV ddaC neurons are severed around APF 5-6 h, and the severed dendrites are cleaned up at around APF 18 h (Lee et al., 2009). Triggered by ecdysone, a steroidal insect molting hormone, ddaC neurons initiate dendrite severing at the proximal positions of dendrites. Upon the binding of EcR-B1 (ecdysone receptor) to ecdysone, two factors Brahma (Brm) and CREB-binding protein (CBP) will activate one of the downstream genes, Sox14, in the class IV da neurons during dendrite pruning (Kirilly et al., 2011). Other molecular pathways are also identified to regulate dendrite pruning; for example, during pruning, Mical a Sox14-targeting gene (Kirilly et al., 2009), the SCF E3 ligase independent of Mical (Wong et al., 2013). Katanin p60-like 1 (Kat-60L1) and Ik2 kinase (Lee et al., 2009). Headcase (hdc) is also required in controlling of dendrite severing (Loncle and Williams, 2012). The removal of pruned dendrites is promoted by local caspase pathway (Williams et al., 2006). Moreover, recent study indicated that compartmentalized calcium transients in different dendritic branches is also essential for the dendrite pruning of class IV da neurons

2

(Kanamori et al., 2013).
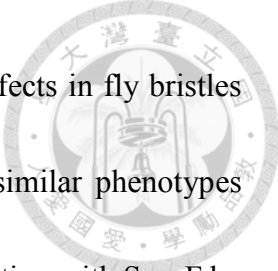
3. The role of IK2 in dendrite pruning

Drosophila Ik2 kinase, a homologue of vertebrate IKK- ε ιν, is one of the members in IκB kinase (IKK) family. These protein kinases are known for participating in innate immune responses in mammalian. DmIKKβ and Ik2 are the two IKK family members in *Drosophila*, DmIKKβ's function is similar to mammalian IKKα protein, participates in innate immune response (Silverman N et al., 2000). However, DmIKKε (Ik2) is important for microskeleton organization and mRNA localization during undergoes oogenesis (Shapiro RS et al., 2006). In recent studies, the Ik2 kinase was identified as an essential protein in dendrite pruning, based on different experiments such as Ik2 RNA interference (RNAi), overexpression of mutant Ik2 and MARCM (mosaic analysis with a repressive cell marker) in class IV da neurons (Lee et al., 2009). Overexpression of Ik2 in lavae neurons causes premature severing of dendrite, indicating the central role of Ik2 in dendrite pruning of class IV da neurons.

4. The role of Spn-F in dendrite pruning

To study how Ik2 regulate dendrite pruning, our group identified a coil-coiled protein, Spn-F, as a good candidate mediator in Ik2 signaling pathway of dendrite pruning (Lin et

3

al., 2015). According to previous studies, Spn-F mutation caused defects in fly bristles and oocytes (Abdu U et al., 2006), and Ik2 mutant flies showed similar phenotypes (Shapiro RS et al., 2006). It also showed that Ik2 has physical association with Spn-F by co-immunoprecipitation experiment. Spn-F can be phosphorylated by Ik2 and this phosphorylaton does not cause Spn-F degradation (Dubin-Bar D et al., 2008). Due to these evidences, during *Drosophila* oogenesis and the morphogenesis of bristle, Ik2 and Spn-F, may participate in the same pathway. In Class IV da neurons, there is likely that Spn-F and Ik2 also act in a similar pathway in dendrite pruning. Our group demonstrated that Spn-F, as a downstream protein of Ik2 signaling pathway, plays an important role in dendrite pruning and links Ik2 to motor protein dynein complex (Lin et al., 2015). In larvae, Spn-F forms puncta in ddaC neurons and these Spn-F puncta disperses in pupal ddaC neurons. This dispersion of Spn-F puncta is dependent on Ik2 activity and the function of motor protein dynein complex. The dispersion of Spn-F puncta is essential for pruning. Spn-F acts as a key role which mediates Ik2/Spn-F/dynein complex formation.

5. Rab11

Rab11, a small G protein, is a member of Ras GTPase superfamily. Previous study revealed that Rab11 localizes at the post-Golgi vesicles, trans-Golgi network (TGN) and the late recycling endosomes, and participates in both endocytic trafficking and exocytic

4

trafficking. Since Rab11 is a G protein, it has two forms: GDP-and GTP-binding forms.

This GDP/GTP transition is regulated by Guanine nucleotide exchange factors (GEFs)

and GTPase-activating proteins (GAPs). The transition and regulation between GDP-and

GTP-binding form of Rab11 plays a key role in regulating of Rab11-dependent vesicle

transport, including the direction and velocity of Rab11-vesicles movements. It is not

clear that how a small G protein regulate these various biological processes in cells. It

was shown that Rab11-vesicles can be transported via microtubules or actin filaments

through the interaction between Rab11 and different adaptor proteins. Thus, by

associating with different adaptors and motor proteins, Rab11-dependent vesicles could

be transported to various subcellular locations.

6. The Aim of this study

Preliminary study in our lab has indicated that class IV da neurons with double-strand

of Rab11 expression showed serious pruning defect at APF 16 h. Due to these data, we

are curious about the role of Rab11 in dendrite pruning. To examine whether the GTPase

activity of Rab11 is required in dendrite pruning, we generated transgenic fly lines

carrying either constitutively active (CA) or dominant negative (DN) mutant Rab11

transgenes and analyzed the pruning defects in these CA- and DN-Rab11 neurons. Next,

we focused on the distribution and movement of Rab11 signals at different time points

after puparium formation in different mutant fly lines. Our previous studies showing that

Spn-F could form complexes with endogenous Rab11 proteins in co-immunoprecipitation

experiments of S2 cells. Thus, we generated a truncated Spn-F construct and try to

identify the Rab11-interacting domain of Spn-F protein by co-immunoprecipitation
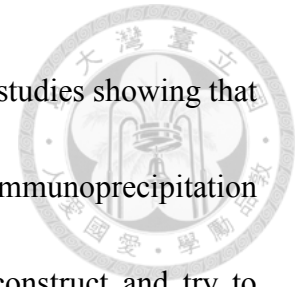
experiment.

Methods

Fly strains

All Drosophila strains used in these experiments are listed in Table 1. For the observation of Class IV da neuron membrane in larva and pupa, ppk-Gal4,UAS-mCD8-GFP and ppk-Gal4,UAS-mCD8-RFP were used. All flies were raised at 25°C.

Confocal imaging

For observation of 3rd instar larval and pupal neuron under confocal (Zensis LSM 700), the larvae were mounted with 90% glycerol on slides and covered by coverslips. Pupae were chosen and put on the slides, high vacuum grease (DOW CORNING) was squeezed between slides and coverslip to reserve some place for pupa for live imagine. The imagines were processed by Zen 2009 software.

APF 16 hour Pupae dissection

First, I used the brush to gently remove the pupae from the vials and put them on the slides and adhered them with the tape. Then used the forceps to remove the puparium operculum gently to let pupa's head expose. Third, removed the puparium operculum and gently caught out the pupae and transferred them to new slides. Pupa were immersed with

7

ddH2O or 90% glycerol, surrounded by high vacuum grease (DOW CORNING), and covered by coverslips for confocal observing.

Construct

The full-length Spn-F was generated from cDNA clone LD01470 (Drosophila Genomics Resource Center) by PCR. To generate Spn-F Δ340-360 truncated protein, the designed primers were used to anneal with full length Spn-F. Then the PCR products were amplified by A-T cloning and the target sequences were isolated by restriction enzymes. Those target sequences were cloned in to PCRII vectors which contained different tags like EGFP, HA, Myc or Flag. The final step was using restriction enzymes to transfer target sequences and tags into pUAST vectors for later experiments.

Cell culture

Our cell line was *Drosophila* S2 cell, and these cells were cultured in full medium which contained Shield and Sang M3 insect medium (Sigma), $KHCO_3$ (AppliChem), yeast extract (Sharlau), bactopeptone (BD) and additional 10% heat-inactivated fetal bovine serum and 1% penicillin-streptomycin (P/S). Our S2 cells were kept in 25ºC, and passaged into next plate in around 3-4 days when the S2 cells were detached. By pipetting the medium up and down and washing up the adherent cells, we could break up the clumps

8

of cells. Then split cells at a 1:2 to 1:4 dilutions in new medium and passaged into new plate.
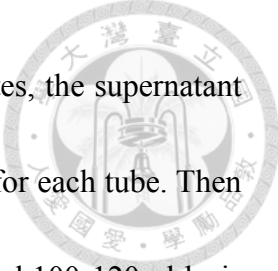
Transfection

S2 cells should be passed into 12 well first for manipulating transfection. In order to efficiently condense DNA, 600 ng of plasmid which contained pUAST vector with the target gene and Tublin-GAL4 were mixed gently with EC buffer and enhancer (QIAGEN). After siting at room temperature for 5 minutes, effectene (QIAGEN) was added. Then gently and quickly vortex the mixture once, and incubated it for per well for 10 minutes at room temperature. Next step was pipetting 600-800 µl medium from the well and gently mixing it with the mixture then adding it back to the well by dropping it slowly and gently. The final step was adding 200 µl new medium to each well and transferring the 12 well plate into 25ºC incubator.

Western blot

After transfection, S2 cells were placed at 25ºC incubator for 40-48 hours. In order to harvest the cells, the S2 cells were washed up by pipetting the medium and transferred to 15cc tube. The cold PBS buffer (137mM NaCl, 2.7mM KCl, 10mM Na_2HPO_4, 2mM KH_2PO_4, pH7.4) was used to wash the rest adherent cells in the well and added it to the

9

15cc tube. Then the tubes were centrifuged at 500g, 4°C for 5 minutes, the supernatant was discarded. Tapped the tube to separate the cells, added 5cc PBS for each tube. Then centrifuged the tubes again. Repeated this step for one time, and added 100-120 μl lysis buffer (pH7.0 20mM Tris buffer, 150mM NaCl, 2mM EDTA, 1% Triton X-100, 10mM PMSF, 10mM beta-glycerol phosphate,1mM Na$_3$VO$_4$, 50mM NaF,1X PNPP phosphatase inhibitor, 1mM DTT) with 1X protein inhibition cocktail. The cell lysates were placed on the shaker at 4°C for 20-25 minutes. Then centrifuged the lysates at 12,000 rpm, 4°C for 12 minutes. The other organelles, membrane, nuclear precipitated at the bottom of the eppendorf. Gently pipetted the supernatant and transferred it to a new eppendorf. Those protein lysates were added with 5X sample buffer which contained pH 6.8 TrisHCl 250%, 4% SDS, 30% Glycerol, 0.02% bromophenol blue. The samples were subjected to SDS-PAGE. After electrophoresis, different proteins were separated in an order by the SDS gel. Then, the proteins in the gel were transferred to PVDF membrane in cold transfer buffer for 90-100 V, 1and a half hour. Transfer buffer contained 25mM Tris, 192mM Glycine, 10% Methanol. We used specific antibody to detect the proteins on the PVDF membrane. First, the membrane was blocked at room temperature with 5% milk reconstituted in PBST (PBS with 0.1% Tween-20) for 1 hour. Second, the membrane was incubated in the 5% milk which contained first antibody overnight at 4°C. The first antibody I had used included: Rabbit anti-C-myc (1:5000), Mouse anti-Flag (1:5000),and Mouse anti-Rab11

(1:2000). Then the first antibody was bound by horseradish peroxidase (HRP)-conjugated anti-Rabbit or anti-Mouse secondary antibodies which were in a 1:5000 dilution for 1 hour at room temperature. In the end, those signals were observed by chemiluminescence (Perkin Elmer).

Co-immunoprecipitation

S2 cells were harvested 40-48 hours after transfecting with Rab11-myc, Spn-F-Flag or truncated Spn-F-Flag. Followed the steps of Western blats, the cell lysates were incubated with 10μl 50% slurry of anti-Flag M2 beads (anti-Flag antibody-conjugated agarose beads, Sigma) with rotation on shaker at 4ºC overnight. The M2 beads were washed first with TBS (50mM Tris-HCl pH7.4, 150mM NaCl), then washed with lysis buffer which was without cocktail. After incubation with M2 beads, the lysates with were precipitated and the supernatants were discarded. The beads with proteins were washed with lysis buffer which was without cocktail for 3 times. Then the precipitated proteins were eluted in 2X sample buffer at 95ºC for 5-10 minutes. The supernatants were loaded into 10-12% SDS bis-acylamide gel once after centrifugation.

Results

Our previous observation that class IV da neurons showed defective dendrite pruning in neurons with Rab11-RNAi expression at APF 16 hrs, suggested a critical role of Rab11 in pruning. To examine whether the GTPase activity of Rab11 is required for dendrite pruning, we generated two types of Rab11 transgenic fly lines. The constitutively active (CA) form of Rab11 has leucine to replace glutamine at the 70th amino acid of Rab11 protein (table 1). The dominant negative (DN) has leucine to replace serine at the 25th amino acid of Rab11 protein.

1. Quantification of the Rab11 expression level in different CA-/DN-Rab11 lines

To quantify the expression level of Rab11-GFP in different transgenic lines. We used confocal microscope to imagine the Rab11-GFP expression in neurons of all CA- and DN-Rab11 lines and calculated the cytosolic mean intensity of Rab11-GFP in the soma of class IV da neurons for each lines by Zen 2009 software (figure 1A). According to the mean intensity of Rab11-GFP signals in different lines, we divided these lines into three groups: weak, medium and strong (figure 1B). We next picked few lines from each group to do the following experiments.

12

2. DN-Rab11 expression affects the dendritic morphogenesis in larval neurons and causes pruning defects in pupal neurons

To examine whether the overexpression of mutant Rab11 proteins could impair the morphogenesis of class IV da neurons in larval, we used class IV da neuron-specific driver line ppk-Gal4 to express either UAS-CA- or UAS-DN-Rab11 together with UAS-mCD8-GFP, which labels the whole plasma membrane of class IV da neurons. By comparing to the wild-type class IV da neurons in larvae (figure 2A), we observed smaller dendritic field at class IV neurons with DN-Rab11 expression (figure 2C), but normal dendritic morphology of neurons with CA-Rab11 expression (figure 2B). It indicated that overexpression of CA-Rab11 does not affect the dendritic development of class IV da neurons, but overexpression of DN-Rab11 reduce the dendritic field of class IV da neurons. Next we examined whether the overexpression of mutant Rab11 could cause pruning defects in class IV da neurons at APF 16 hrs. We observe strong pruning defects in class IV da neurons with DN-Rab11 expression (table 3, figure 2D&F), but weak pruning defects in neurons with CA-Rab11 expression (table 3, figure 2E&F). The pruning defects caused by DN-Rab11 expression were stronger in neurons with strong ppk-GAL4 line (on chromosome II) than the one with weak ppk-GAL4 line (on chromosome III) (table 3A&B), indicating the positive correlation between the pruning phenotypes and DN-Rab11 protein expression amounts. In order to rule out the possibility
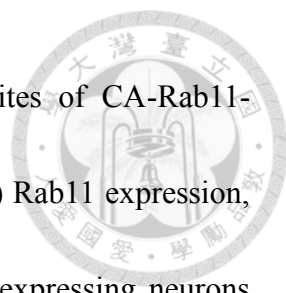
13

that non-specific effects caused by transgene insertion, we crossed UAS-DN-Rab11[3-4] line with ppk-eGFP line and examined pruning phenotypes. We did not detect pruning defects in neurons of UAS-DN-Rab11[3-4] line without ppk-GAL4 driver (table 3C), suggesting that the pruning defects observed in class IV da neurons is GAL4-dependent.

3. The observation of Rab11 in C4da neurons of early pupae

Previous studies showed that Rab11 signals appeared in proximal dendrites of C4da neurons of pupae. To further study the movement of Rab11 signals in class IV da neurons, we performed live imaging of wild-type Rab11-GFP signals in neurons by confocal microscopy at different time points. We could detect Rab11s in the soma and proximal dendrites, and often observed Rab11-GFP signals appearing at the branches of dendrites (figure 3).
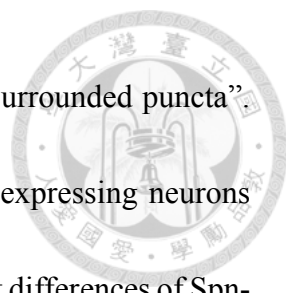
After 4 hour APF, we observe enriched Rab11-GFP accumulated in large, globular structures, which are called varicosities (figure 4). Those varicosities often appeared at the branches and around the dendrite thinning sites (figure 4). We also performed live imaging in neurons with either CA-Rab11 or DN-Rab11 expression. We could observe the GFP-enriched varicosities in the dendrites of class IV da neurons with CA-Rab11 expression (figure 5B), but not the ones with DN-Rab11 expression (figure 5C). Moreover, we quantified the number of varicosity formation in dendrites of class IV da

14

neurons at APF 7 hrs. The number of varicosities in the dendrites of CA-Rab11-expressing neurons are comparable to the cells with wild-type (WT) Rab11 expression, but almost no varicosity formation in the dendrites of DN-Rab11-expressing neurons (figure 5C&D).
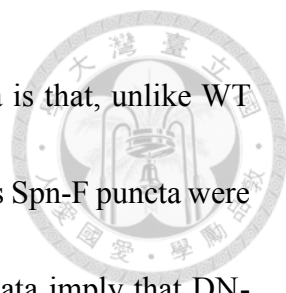
4. The observation of Rab11 and Spn-F signals in larva C4da neurons

According to previous studies, Spn-F showed some colocalization with wild-type Rab11, in class IV da neurons. To further characterize the colocalization of Rab11 and Spn-F in neurons, we expressed Spn-F-mCherry and eGFP-Rab11 protein in larva Class IV da neuron and analyzed the Spn-F puncta number, size and the colocolization with WT-, CA-, DN-Rab11 signal in cell body (figure 6). All imagines were collected by z-stacking. In order to have a clear characterization of the association between Spn-F and Rab11, we categorized these puncta into "colocalized", "touched", "surrounded", and "non-associated" puncta. When two puncta appeared on the same section layer of image and the highest peaks of two colors showed overlapped, we called it "colocalized puncta". If two puncta appeared very close on the same section of image, but the peaks of two signals only showed partially overlapping, or these two puncta were in same position but on the adjacent section layers, we would call it "touched puncta". If one was surrounded

15

by the other punctum on the same section layer, we would call it "surrounded puncta".

The number of Spn-F puncta significantly increased in DN-Ran11-expressing neurons

compared to WT- or CA-Rab11-expressing neurons, but no significant differences of Spn-

F punctum number were observed between WT- and CA-Rab11-expressing neurons

(figure 6C). We also calculated the diameter of each Spn-F puncta and grouped then in to

five categories: less than 0.6 μm, 0.6-1.0 μm, 1.0-1.3 μm, 1.3-1.6 μm, more than 1.6 μm

in WT-, CA- and DN-Rab11-expressing neurons (figure 6D). In all WT-, CA- and DN-

Rab11-expressing neurons, small Spn-F puncta were most abundant, but Spn-F puncta in

DN-Rab11 overexpressing neurons showed higher number in small size puncta (diameter

less than 0.6 μm and 0.6-1.0 μm) compared to WT and CA (figure 6D). In order to

characterize the association between Spn-F and Rab11 puncta, we calculated the number

of "colocalized puncta", "touched puncta", "surrounded puncta". According to the

analysis of puncta size distribution about these three Spn-F puncta group, "colocalized"

puncta had higher proportion of small Spn-F puncta (diameter less than 0.6 μm and 0.6-

1.0 μm), and the "touched" puncta had more big puncta proportion (1-1.3 μm or more

than 1.6 μm) in all WT, CA and DN-Rab11 neurons. It suggested that maybe small Spn-

F puncta were more likely to colocalize with Rab11 signals. We also observed that DN-

Rab11-expressing neurons showed more number of "colocalized", "touched" and

"surrounded" Spn-F puncta than WT or CA-Rab11 neurons. One possible explanation for

16

the increased number of "touched" and "surrounded" Spn-F puncta is that, unlike WT and CA-Rab11 signals, DN-Rab11 is more dispersed in cell body, thus Spn-F puncta were more likely to be surrounded or touched by Rab11 signals. These data imply that DN-Rab11 has a better association with Spn-F protein, that is consistent with our previous co-IP studies.

5. The movement of Rab11 signals in C4da neurons at early after puparium formation (APF)

To study the signal movement of Rab11, I took confocal imagines of WT-, CA- and DN-Rab11-expressing C4da neurons every 5-15 minutes and observed that Rab11 showed movement in all three types of neurons (figure 7). The signals of all Rab11-GFP are dynamic and often observed enriched at dendrite branch sites. Furthermore, I examined the movement of Rab11-GFP in class IV da neurons with either Spn-F-RNAi, Ik2-RNAi, or Dynein heavy chain (Dhc)-RNAi, and found out that Rab11 showed movement on dendrites and enrichment at branches (figure 8A-C). We didn't detect any differences among the movement of WT-, CA- and DN-Rab11 signals in dendrites of class IV da neurons at early pupal stages, even after we shortened the intervals between image acquisition to 5-10 seconds.

6. Quantification of vesicle movement in C4da neurons at early after puparium formation (APF)

One possibility that we could not find the difference of Rab11 signals in the dendrites of control and mutant neurons is that the moving speed of Rab11 signals is too fast to defect. Therefore, we used the ZEISS light microscope Axio Observer.Z1 (From Ya-Wen Liu lab) and Axio Imager.M2 (From Chun-Liang Pan lab) to observe the Rab11 movement at the interval of 1 second. Using the ZEISS light microscope at the interval of one second, we could detect the movement of Rab11 vesicles in the dendrite, in spite of the low resolution of acquired images. The kymograph of Rab11-vesicle movement in 30 seconds showed bi-directional movement (figure 9A). We noticed that there were some big Rab11-dependent vesicles at branches especially at the first branch, and they rarely move. We called this big, non-moving vesicle as "immobile big Rab11 vesicle", compared to the fast-moving, small Rab11 vesicle, which is called "mobile small Rab11 vesicle". In WT or CA-Rab11 overexpressing neurons, we observed obvious vesicles signal compared to DN-Rab11 overexpressing neurons. Due to the fact that active form Rab11 regulates vesicles formation, we couldn't observe vesicles in DN-Rab11 overexpression neurons. DN-Rab11 signals were quite dispersed so we cannot analyze the DN-Rab11 vesicle movement and speed. In contrast, we observed that many Rab11-vesicles appeared at CA-Rab11 overexpression neurons. We calculated the number of vesicles

18

passing through one slice in 2 minutes, and the number in CA-Rab11 neurons was over

40 which significantly higher than WT-Rab11 and IK2-RNAi neurons (figure 9D). Next,

we analyzed the speed of Rab11 vesicles in WT, CA-Rab11 overexpression neurons and

also Ik2 knock down neurons, and we divided the vesicles into two groups: "moving in"

and "moving out" groups by moving direction of vesicles transport. These data were

quantified by Zen 2012 software and MetaMorph offline imagine processing software. In

"moving out" group, the average speed of WT-Rab11 vesicles was 0.7133 µm/s, and there

was no significant difference between WT, CA or IK2-RNAi. However, the CA-Rab11

vesicles transported significantly faster compared to WT or IK2-RNAi in "moving in"

group (figure 9). Those Rab11-dependent vesicles in WT, CA or IK2-RNAi had no

significant difference in vesicle sizes, characterized by analyzing the diameter of Rab11

vesicles (figure 9).

7. Spn-FΔ340-364 (D16) truncation disturbed the association between Spn-F and Rab11

Previous data showed that Spn-F had association with endogenous Rab11 protein in S2

cells. Full length Spn-F contains three coil-coiled (CC) domains and a Spn-F conserved

domain (SCD) (figure 10A). Previous studies showed that SCD domain might play a

critical role of associating with Rab11. To further characterize the specific Rab11-

19

associating domain of Spn-F, we generated Spn-F △340-364 (D16) construct and used

Drosophila S2 cell for transfection. By co-immunoprecipitation, we characterized that the

△340-364 truncation of Spn-F would disturb the association with Rab11, but not totally

deleted the interaction (figure 10B).
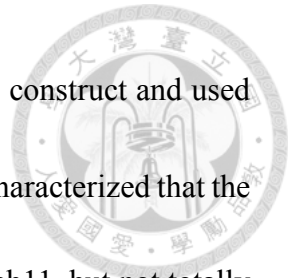
Discussion

1.   **The association of Spn-F and Rab11 in cell body in larva**

Although Spn-F and Rab11 can form complexes in the co-immunoprecipitation experiment of S2 cell, we did observe colocalization of Spn-F and Rab11 in some, but not all class IV da neurons. One possibility is that when we overexpress Spn-F and Rab11 at the same time causes abnormal defects. There were abundant Spn-F that caused them interacted with themselves instead of with Rab11 proteins. Another possibility is that we separated these data into more careful classification, and analyzed every neuron and found the signal peak. These imagines were taken by z-stacking but not by snap shot so we could observe more details about the association between Spn-F puncta and Rab11 puncta (figure 6). Interestingly, we observed more small Spn-F puncta (diameter less than 0.6 μm and 0.6-1.0 μm) appeared in DN-Rab11-expressing neurons, compared to WT and CA-Rab11-expressing neurons. It raises a possibility that Spn-F might have a stronger interaction with DN-Rab11 than with itself. We also tried to observe the association between Rab11 and Spn-F in dendrites at APF 5-7 hrs, when most of the varicosities are formed. Due to the dispersion of Spn-F signals, it was very difficult to observe Spn-F signals at varicosities because the signals were too weak. These data suggest that the DN-Rab11 has greater association with Spn-F puncta not only in vitro but also in neurons.

21

2. Analysis of Rab11-dependent vesicles

In this study, we compared the speed and vesicle number of Rab11 in WT, CA-Rab11-expressing neurons and Ik2 knockdown neurons. We also took imagines of DN-Rab11 neurons, Spn-F and dynein heavy chain knockdown neurons. However, the signals in these neuron were very dispersed and we could barely observed Rab11-depent vesicles. Besides those small, moving Rab11-dependent vesicles, we also observe immobile big Rab11 signals appeared at branches where many Rab11-dependent vesicles passing through. We assumed that these big signals play a role just like recycling endosomes, which regulates small Rab11-dependent vesicles transporting in and out. The dynamic signals from confocal imagines that accumulated at branches were assumed to be caused by these small mobile vesicles moving through the immobile Rab11 signals. Further studies are required to elaborate how these immobile big Rab11-dependent vesicles function during neuron development. At the proximal dendrite of class IV da neurons, 90% of microtubules are minus-end pointing out from the soma. The cytoplasmic dynein complexes move toward the minus ends of microtubules, but kinesins move toward the plus ends. Therefore, the moving small Rab11 vesicles observed in the proximal dendrites could be transported by both dynein or kinesin. According to other studies, the velocity of recombinant Rab11-FIP3-dynein-dynactin motor complex in vitro has been characterized (McKenney RJ. et al., 2014). The average velocity is 0.594 ± 0.192 μm/s,

22

but the distribution ranges from 0.3-1.2 μm/s and the maximal velocity reaches almost

1.3 μm/s. However, the velocity of purified kinesin ranges from 0.16 μm/s to 0.85 μm/s

at different concentration of ATP and kinesin and the maximal velocity also reaches over

1 μm/s (Xu J. et al., 2012) and the velocity will change if there are two or more motor

proteins carry a same vesicle. In our data, the velocity of Rab11-dependent vesicles

transported out of the cell body is 0.713 ± 0.239 μm/s, which ranges from 0.33 μm/s to

1.06 μm/s. The velocity of vesicles transported in is 0.522 ± 0.169 μm/s and it ranges

from 0.33 μm/s to 0.88 μm/s. It seems like the velocity of vesicles transported in the cell

body is lower, and 90% of the microtubules are minus-end pointing out from the cell body,

thus this difference probably caused by the velocity of kinesin. It is really hard to

determine which motor protein carries Rab11-dependent vesicles in our study, at least we

can say the velocity we analyzed is compatible to the previous studies. However, in CA-

Rab11 overexpressing neuron, the vesicles transported in the cell body were faster than

WT-Rab11 vesicles but there was no significance between WT and CA-Rab11 in

transported in group. We assumed that since dynein associates with Rab11-GTP, most

CA-Rab11 vesicles were carried by dynein. The velocity of two directions were non-

significant (p value = 0.3810). We could characterize the average velocity of dynein in

dendrites is 0.893 ± 0.271 μm/s no matter the direction. The WT-Rab11 vesicles

transported in to the cell body were slower than CA-Rab11 vesicles may because some

23

of the WT-Rab11 vesicles were carried by kinesin. In the transported out group, there is

possibility that most of WT-Rab11 vesicles were carried by dynein due to non-

significance between WT and CA-Rab11 neurons.
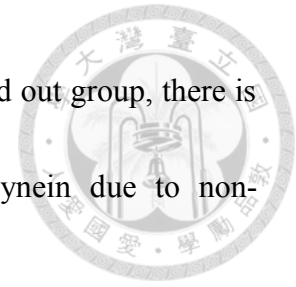
3. Local endocytosis and varicosity formation

Rab5 had been showed to regulate local endocytosis at the dendrite severing sides. These

Rab5-dependent endosomes were transported to two sides of the severing side and

accumulated (Kanamori, T. et al., 2015.). However, it is still unknown which molecule

plays the role in recycling these endosomes to the membrane and forms varicosities. In

our study, we observed Rab11 accumulates in the varicosities. In cells, Rab11 locates at

recycling endosome (RE) and regulates late endosomes recycling (Tobias Welz et al.,

2014). Due to these evidences, we suggested that Rab11 may participate in recycling

those vesicles to the membrane and increase the membrane volume and form varicosities

(figure 11).

Reference

Puram, S. V., and Bonni, A. (2013) Cell-intrinsic drivers of dendrite morphogenesis. *Development (Cambridge, England)*, 140(23):4657–4671.

Luo L and O'Leary D.D. (2005) Axon retraction and degeneration in development and disease. *Annu. Rev. Neurosci* 28:127–156.

M. Schubiger, A.A. Wade, G.E. Carney, J.W. Truman, M. Bender (1998) Drosophila EcR-B ecdysone receptor isoforms are required for larval molting and for neuron remodeling during metamorphosis. *Development* 125(11):2053-62.

Truman JW (1990) Metamorphosis of the central nervous system of Drosophila. *J Neurobiol* 21(7):1072-84.

Awasaki T, Ito K (2004) Engulfing action of glial cells is required for programmed axon pruning during Drosophila metamorphosis. *Curr Biol* 14(8):668-77.

Williams DW, Truman JW (2005) Cellular mechanisms of dendrite pruning in Drosophila: insights from in vivo time-lapse of remodeling dendritic arborizing sensory neurons. *Development* 132(16):3631-42. Epub 2005 Jul 20.

Lee HH, Jan LY, Jan YN (2009) Drosophila IKK-related kinase Ik2 and Katanin p60-like 1 regulate dendrite pruning of sensory neuron during metamorphosis. Proc Natl Acad Sci U S A 106(15): 6363–6368.
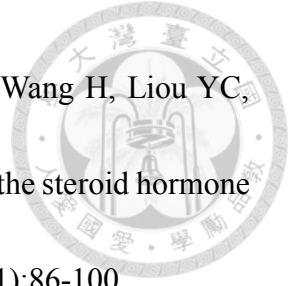
Kirilly D, Wong JJ, Lim EK, Wang Y, Zhang H, Wang C, Liao Q, Wang H, Liou YC, Wang H, Yu F (2011) Intrinsic epigenetic factors cooperate with the steroid hormone ecdysone to govern dendrite pruning in Drosophila. *Neuron* 72(1):86-100.

Kirilly D, Gu Y, Huang Y, Wu Z, Bashirullah A, Low BC, Kolodkin AL, Wang H, Yu F (2009) A genetic pathway composed of Sox14 and Mical governs severing of dendrites during pruning. *Nature Neuroscience* 12: 1497-1505.

Wong JJ, Li S, Lim EK, Wang Y, Wang C, Zhang H, Kirilly D, Wu C, Liou YC, Wang H, Yu F (2013) A Cullin1-based SCF E3 ubiquitin ligase targets the InR/PI3K/TOR pathway to regulate neuronal pruning. *PLoS Biol* 11(9):e1001657.

Loncle N, Williams DW (2012) An interaction screen identifies headcase as a regulator of large-scale pruning. *J Neurosci* 32(48):17086-96.

Williams DW, Kondo S, Krzyzanowska A, Hiromi Y, Truman JW (2006) Local caspase activity directs ngulfment of dendrites during pruning. *Nat Neurosci* 9: 1234–1236.

Kanamori T, Kanai MI, Dairyo Y, Yasunaga K, Morikawa RK, Emoto K (2013) Compartmentalized calcium ransients trigger dendrite pruning in Drosophila sensory neurons. *Science* 340: 1475–1478.

Silverman N., Zhou R., Stöven S., Pandey N., Hultmark D., ManiatisT (2000) A Drosophila IκB kinase complex required for Relish cleavage and antibacterial immunity. *Genes & Dev* 14:2461–2471.

Shapiro RS, Anderson KV (2006). Drosophila Ik2, a member of the I kappa B kinase family, is required for mRNA localization during oogenesis. *Development* 133(8):1467-75.

Lin T, Pan PY, Lai YT, Chiang KW, Hsieh HL, Wu YP, Ke JM, Lee MC, Liao SS, Shih HT, Tang CY, Yang SB, Cheng HC, Wu JT, Jan YN, Lee HH (2015) Spindle-F Is the Central Mediator of Ik2 Kinase-Dependent Dendrite Pruning in Drosophila Sensory Neurons. *PLoS Genet* 11(11):e1005642.

Abdu U., Bar D. and Schüpbach T (2006). Spn-F encodes a novel protein that affects oocyte patterning and bristle morphology in Drosophila. Development 133, 1477-1484.

Dubin-Bar, D., Bitan, A., Bakhrat, A., Kaiden-Hasson, R., Etzion, S., Shaanan, B., & Abdu, U (2008). The Drosophila IKK-related kinase (Ik2) and Spindle-F proteins are part of a complex that regulates cytoskeleton organization during oogenesis. *BMC Cell Biology* 9, 51.

Welz T, Wellbourne-Wood J, Kerkhoff E (2014) Orchestration of cell surface proteins by Rab11. *Trends Cell Biol*.24(7):407-15.

Otani T, Oshima K, Onishi S, Takeda M, Shinmyozu K, Yonemura S, Hayashi S (2011) IKKε regulates cell elongation through recycling endosome shuttling. *Dev Cell* 20(2):219-32.

Kanamori T, Yoshino J, Yasunaga K, Dairyo Y, Emoto K (2015) Local endocytosis triggers dendritic thinning and pruning in Drosophila sensory neurons. *Nat Commun* 6:6515.

Richard J. McKenney, Walter Huynh, Marvin E. Tanenbaum, Gira Bhabha, Ronald D. Vale (2014) Activation of cytoplasmic dynein motility by dynactin-cargo adapter complexes. *Science* 345(6194):337-41.

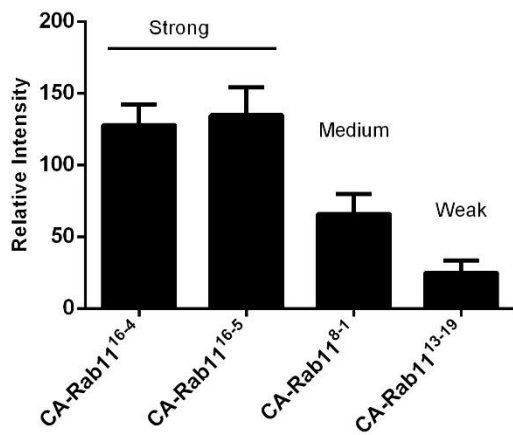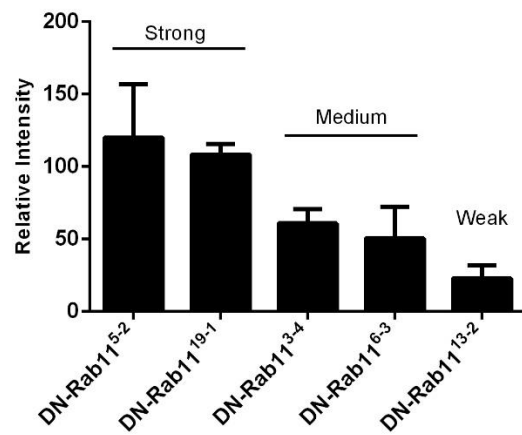Xu J, Shu Z, King SJ, Gross SP. (2012) Tuning multiple motor travel via single motor velocity. *Traffic* (9):1198-205.

Figure

Figure 1

ppk>CA-Rab11$^{16\text{-}3}$-GFP
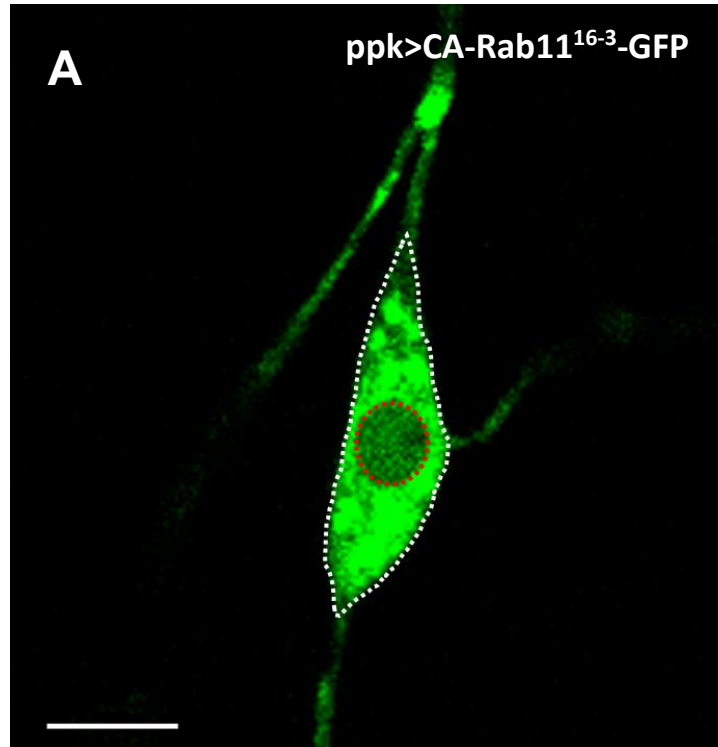
Cytosolic mean signal intensity =

$$\frac{\text{Total intensity of whole cell body- Total intensity of nucleus}}{\text{Cell body – nuclear area}}$$

29

Figure 1. Quantification of soma Rab11 signal intensity in Class IV da neuron

(A) A confocal imagine of third instar larvae neuron of ppk>CA-Rab11[16-3]-GFP. The signals in soma were quantified (The area between white dotted line and red dotted line). White dotted line represents the whole cell body area, and the red dotted line represents the nuclear area. These data were quantified by Zen 2009 software. The area in the red dotted line represents nucleus and the area in the white dotted line represents cell body. The scale bar represents 10μm. (B-C) Relative intensity of Rab11 signals in different CA and DN fly lines. These data were categorized in three groups: Strong (relative intensity >100), Medium (relative intensity is between 50-100) and Weak (relative intensity <50).

Figure 2

third instar larva

W1118	ppk>CA-Rab11$^{8-1}$-GFP	ppk>DN-Rab11$^{3-4}$-GFP
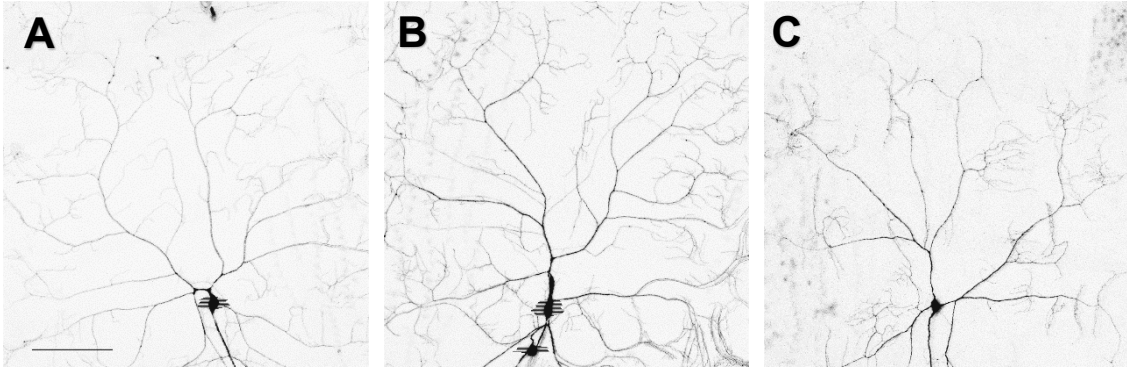
Pupa 16h APF

ppk>DN-Rab11$^{3-4}$-GFP	ppk>CA-Rab11$^{8-1}$-GFP

31
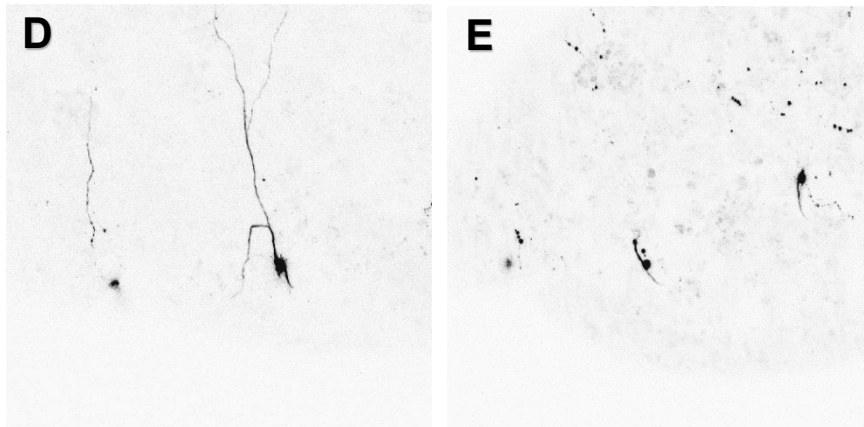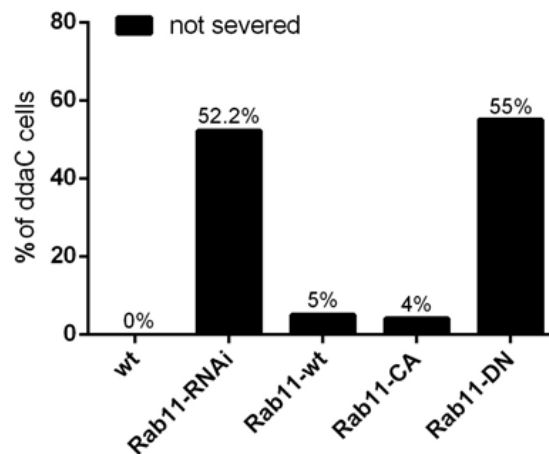
Figure 2. The morphology and pruning defects of class IV da neurons in mutant

Rab11 strains.

(A-E) Neuron morphology of WT, CA and DN-Rab11 overexpress neurons in third instar larva by confocal. The neurons were visualized with *ppk-Gal4,UAS-mCD8-GFP*. (A)W1118 (B) CA-Rab11 and (C) DN-Rab11 overexpression were driven by ppk-GAL4. The scale bar represents 100μm. (D-F) Class IV da neurons were observed at APF 16 hrs after pupae dissection. (D) DN-Rab11 (E) CA-Rab11 overexpression were driven by ppk-GAL4. DN-Rab11 neuron showed pruning defect, the proximal dendrite wasn't severed. CA-Rab11 neuron was pruned at APF 16 hrs. (F) Analysis of pruning defect percentage in different strains. More than a half of neurons showed pruning defect in Rab11 knockdown and DN-Rab11 overexpression conditions.

32

Figure 3

ppk>WT-Rab11³⁻¹-GFP
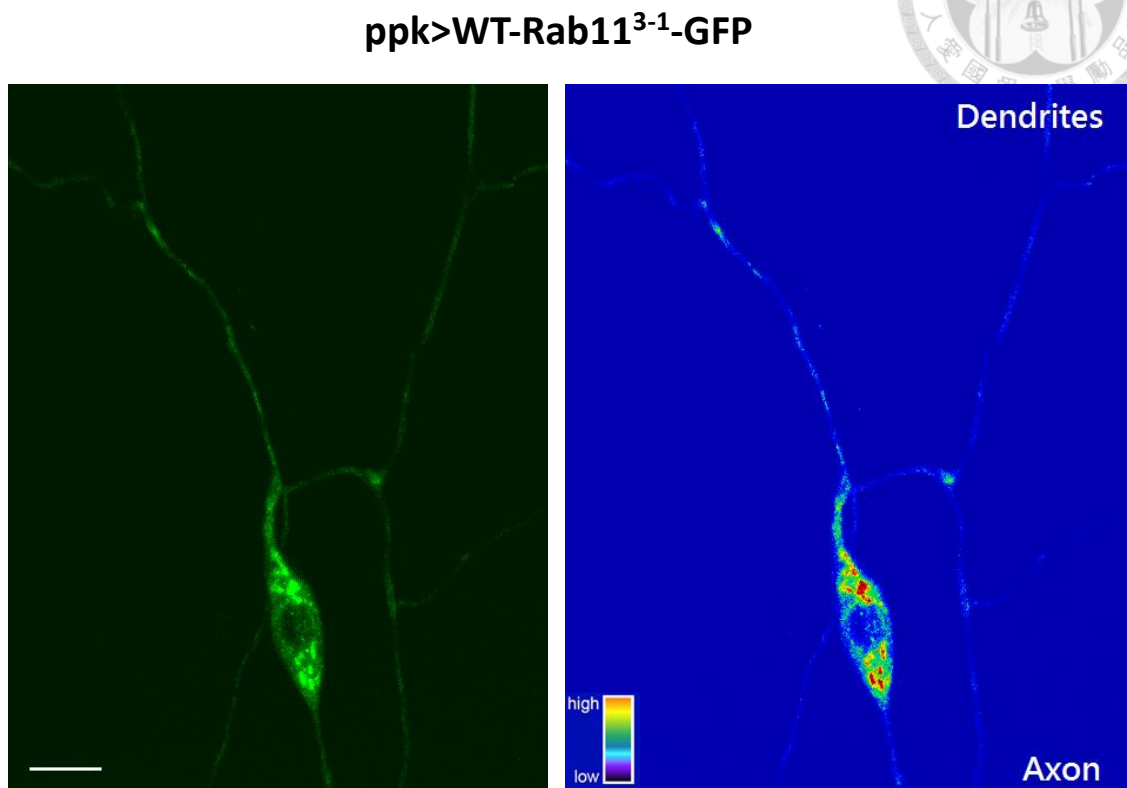
Figure 3. The Rab11 signals distribution in eGFP tagged wild type Rab11 overexpression line at early APF.

A confocal z-stacking imagine of WT-Rab11-GFP overexpression ddaC neuron. The neuron was visualized with *ppk-Gal4,UAS-mCD8-RFP*. WT-Rab11-GFP signals were classified in rainbow color by Zen 2009 software. Rab11 signals appeared at proximal dendrite and somehow enriched at the branches in Class IV da neurons. 82.35% of WT-Rab11 overexpression neurons shown these signal enrichments at the branch sides (n= 17, these data were taken for 1-2 minutes at early APF by ZEISS Light Microscope Axio Observer.Z1 and Axio Imager.M2). The scale bar represents 10μm.

33
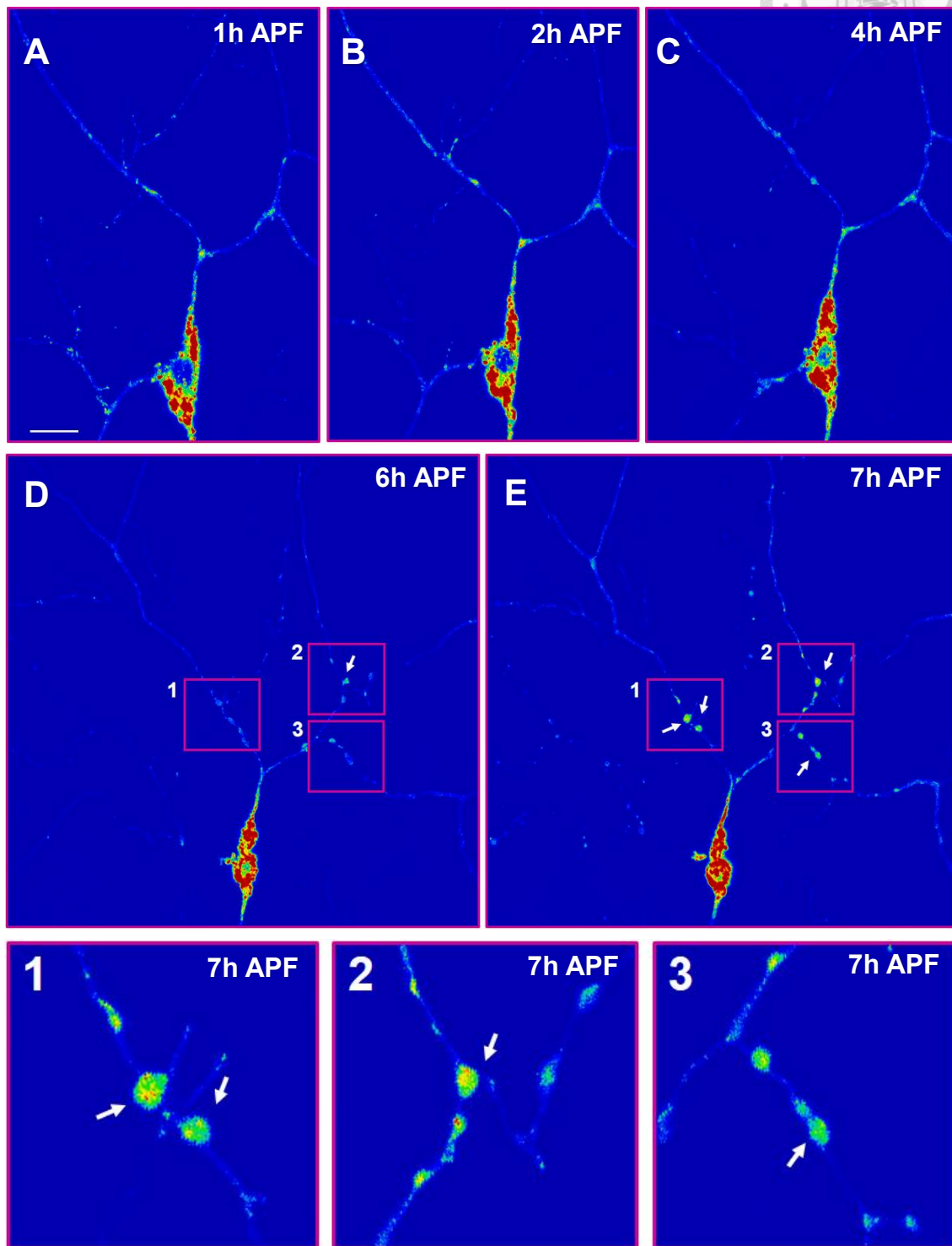
Figure 4

Figure 4. The Rab11 signals distribution in Wild type Rab11 overexpression neuron at 1-7 hrs APF.

(A-E) Confocal z-stacking pictures taken at 1,2,4,6 and 7 APF. The neuron was visualized with *ppk-Gal4,UAS-mCD8-RFP*. The scale bar represents 10μm. WT-Rab11-GFP signals were classified in rainbow color by Zen 2009 software. (A-C) The distribution of WT-Rab11-GFP signals was shown. These signals appeared at branches and also proximal dendrite. (D-E) Varicosities started to appear after 4-5h APF (white arrow heads). (E) Obvious varicosities formed at 7h APF (1-3 square, white arrow heads). WT-Rab11-GFP signals showed enrichment at varicosities.

Figure 5

A   **ppk>WT-Rab11$^{3\text{-}1}$-GFP**

B   **ppk>CA-Rab11$^{8\text{-}1}$-GFP**

36
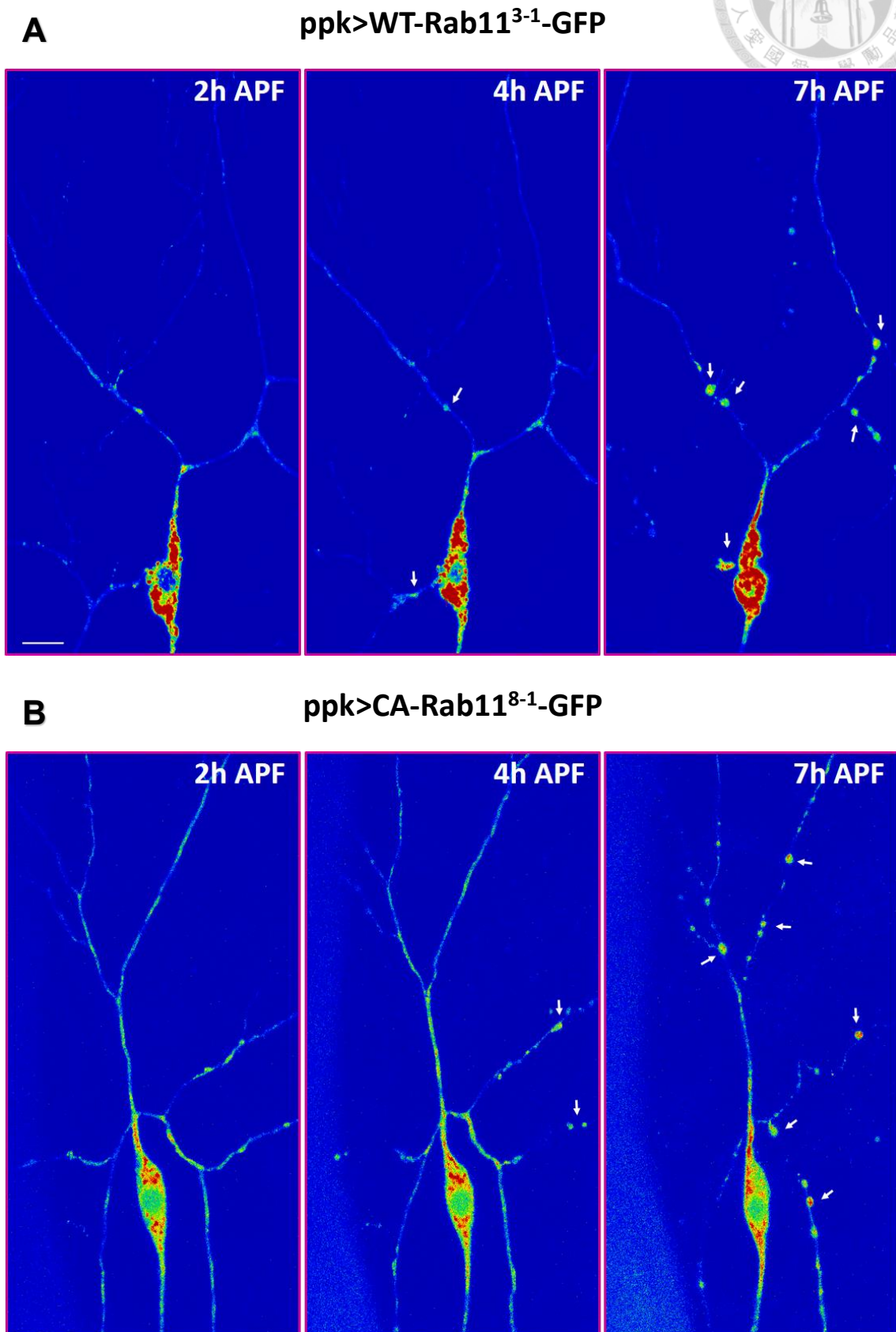
**C**

ppk>DN-Rab11^{6-3}-GFP
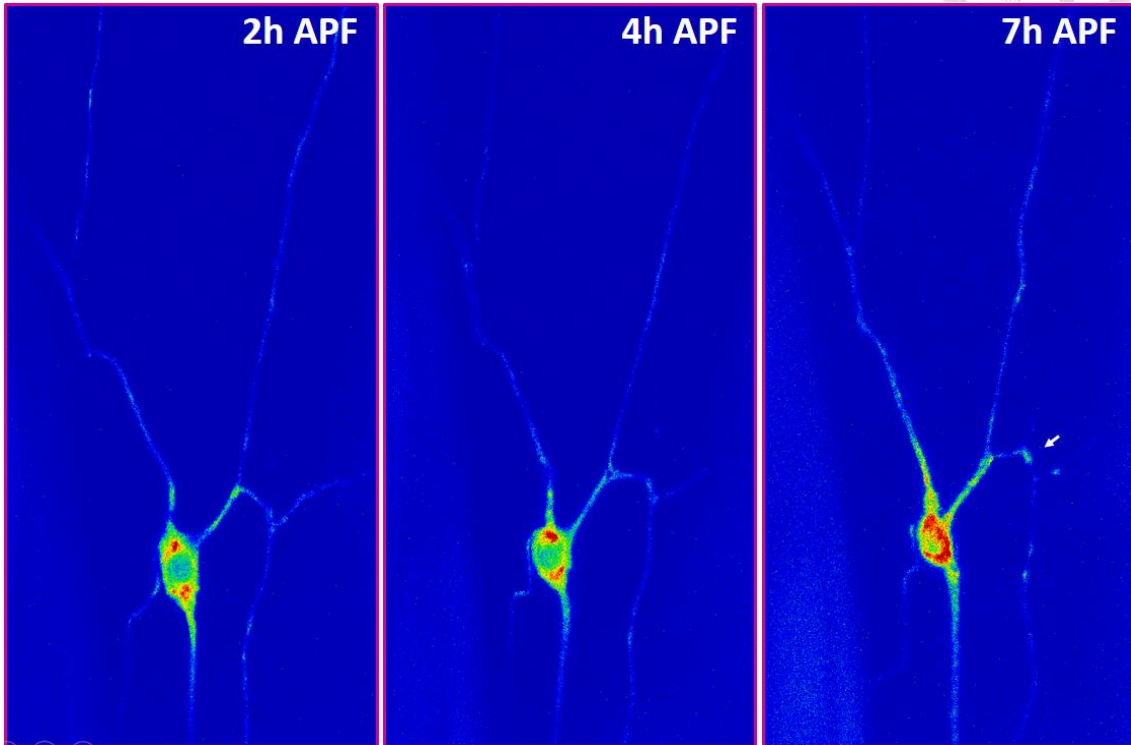
D
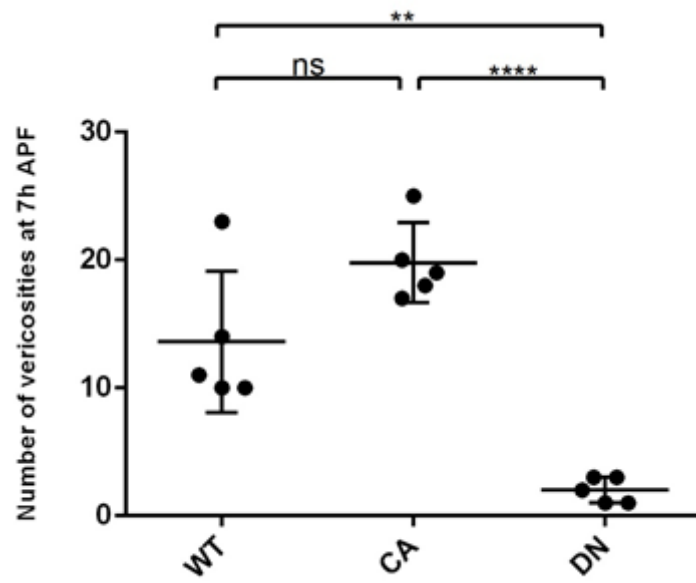
**Figure 5. Quantification of varicosities in WT, CA, DN-Rab11 overexpression lines at 2-7 hrs APF.**
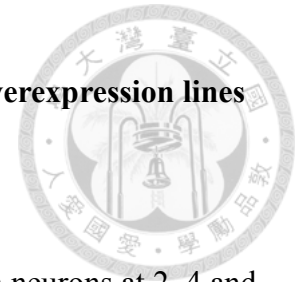
(A-C) Confocal imagines of WT, CA and DN Rab11 overexpression neurons at 2, 4 and 7 hrs APF. The neuron was visualized with *ppk-Gal4,UAS-mCD8-RFP*. WT-Rab11-GFP signals were classified in rainbow color by Zen 2009 software. More varicosities formed in CA Rab11 overexpression neurons, and nearly none formed in DN Rab11 overexpression neurons. The scale bar represents 10μm. (D) Quantification of the varicosities number at 7h APF of WT, CA and DN Rab11 overexpression neurons. There were significances between WT/DN neurons and CA/DN neurons. A varicosity was counted when the membrane became globular and WT-Rab11-GFP enrichment occurred.
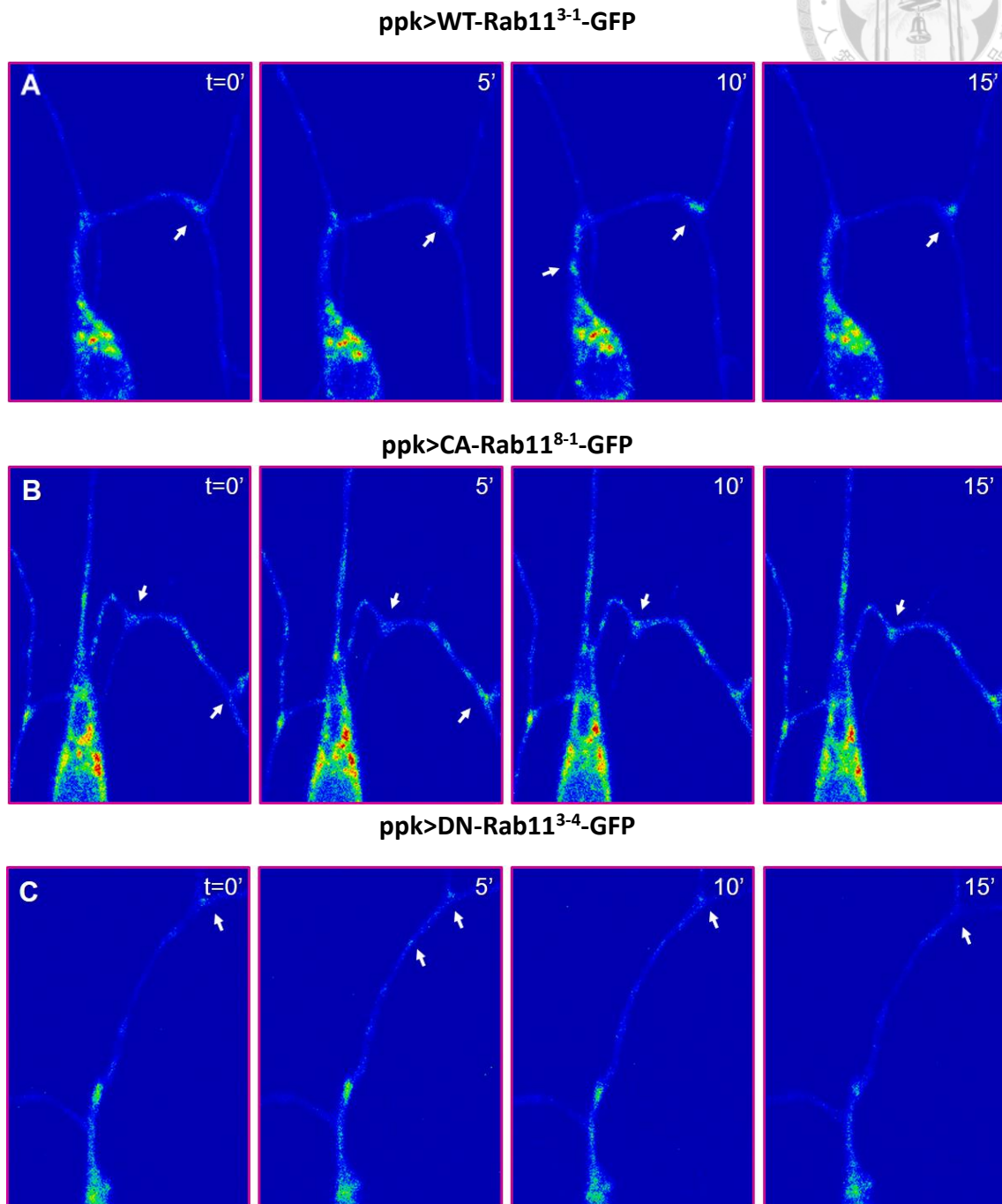
Figure 6
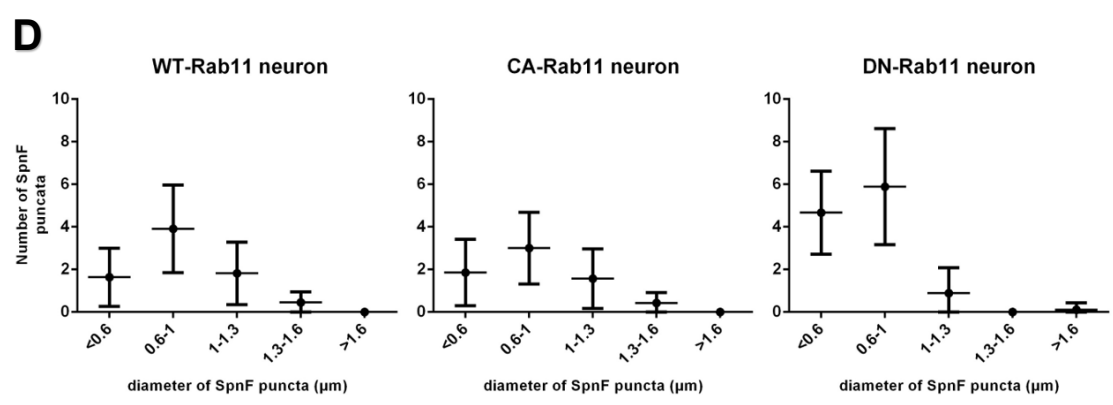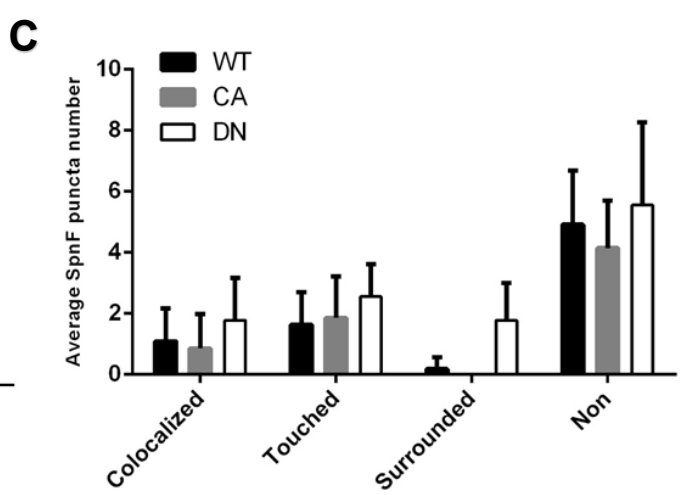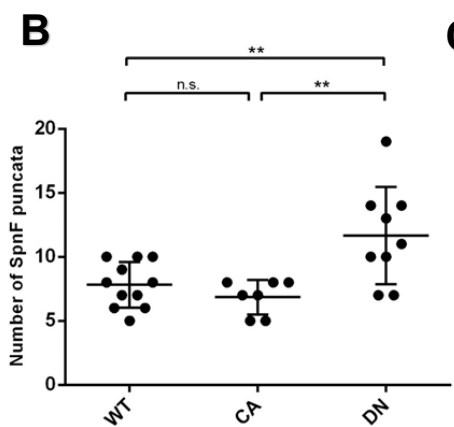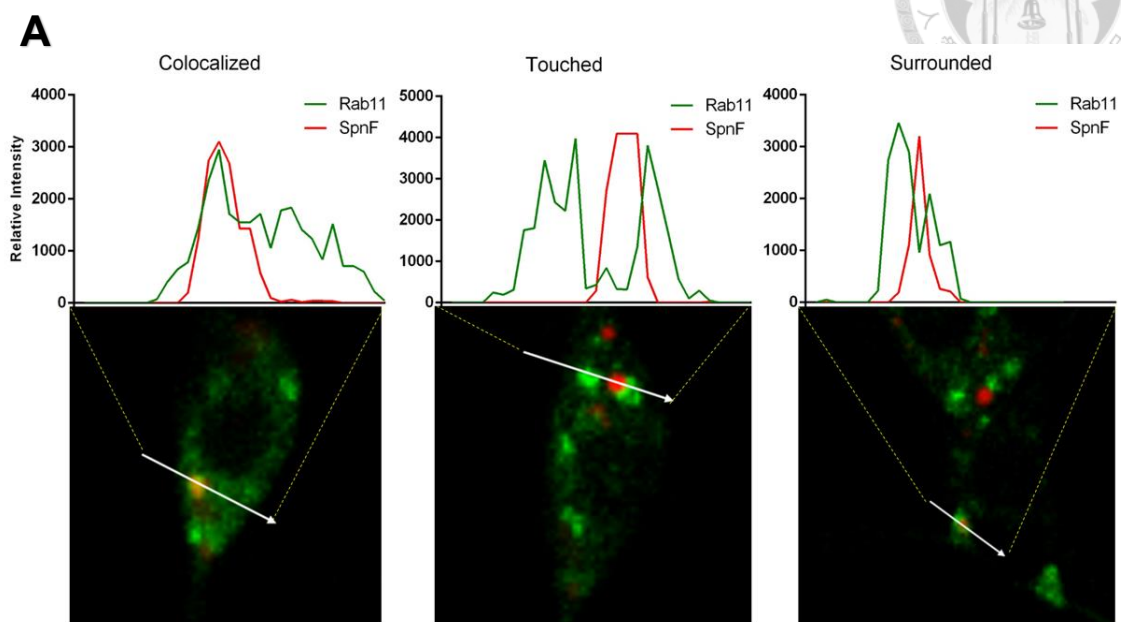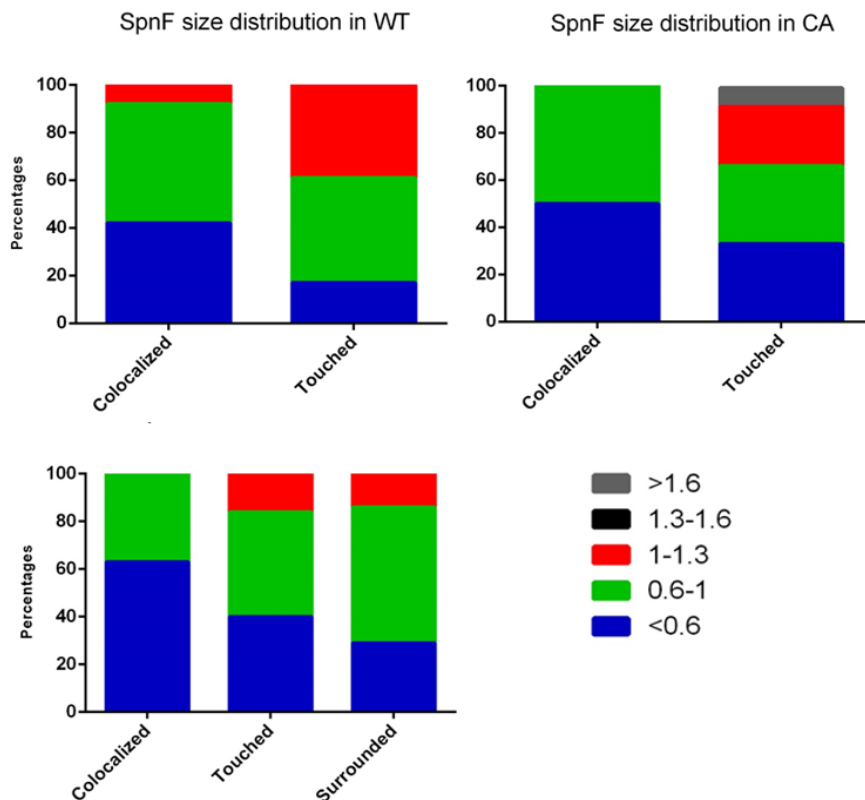
Figure 6. Distribution of Spn-F and Rab11 signals in the cell body of third instar larva neurons.

(A)The signal chart of Rab11 and Spn-F from white arrow line in three association group "colocalized", "touched" and "surrounded" Spn-F puncta. Rab11 and Spn-F signal peak were overlapped at same spot in "colocalized" group. In "touched" group, the Rab11 peak was near Spn-F peak and was surrounded by Rab11 signal peak in "surrounded" group.

(B) Analysis of number of Spn-F puncta in WT, CA and DN-Rab11 neuron. (C) Average Spn-F puncta number in three groups in WT, CA and DN-Rab11 neuron. (D) Size distribution of Spn-F puncta in WT, CA and DN-Rab11 neuron. (E) Size distribution of Spn-F puncta in each group in WT, CA and DN-Rab11 neuron.

40

Figure 7

ppk>WT-Rab11³⁻¹-GFP


ppk>CA-Rab11⁸⁻¹-GFP

ppk>DN-Rab11³⁻⁴-GFP

Figure 7. Movement of WT-, CA- and DN-Rab11 in class IV da neuron at early APF.
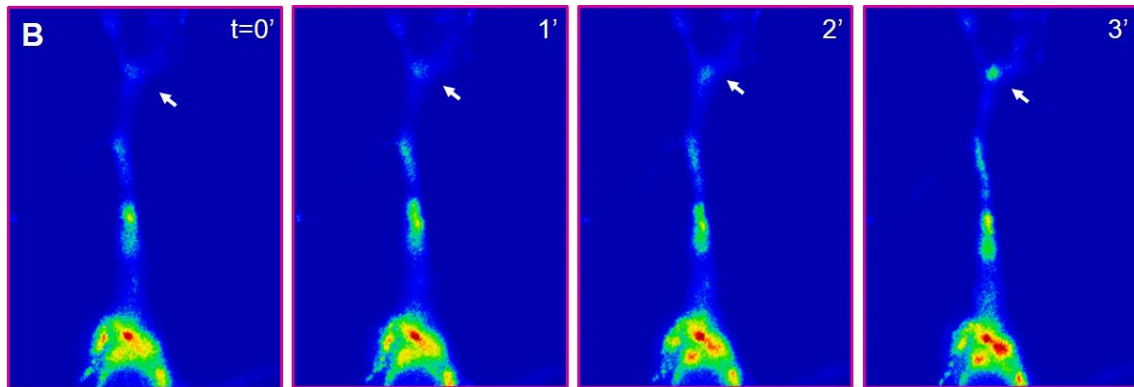
(A-C) Imagines of WT, CA and DN Rab11 overexpression neurons at early APF (1-2 hrs APF). The neuron was visualized with *ppk-Gal4,UAS-mCD8-RFP*. WT-Rab11-GFP signals were classified in rainbow color by Zen 2009 software. Rab11 showed movement on dendrites and variety at branches. (A) ppk>WT-Rab11[3-1]-GFP (B) ppk>CA-Rab11[8-1]-GFP (C) ppk>DN-Rab11[3-4]-GFP in ddaC neurons at early APF. The scale bar represents 10μm.
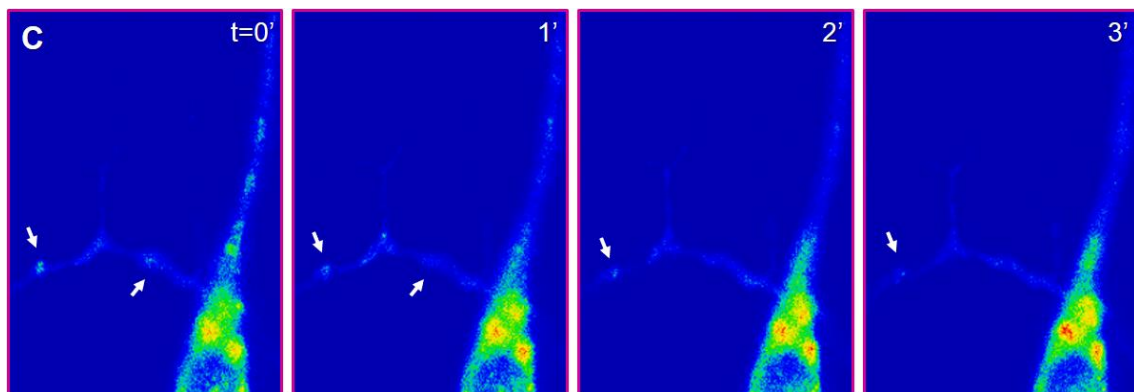
42

Figure 8

Spn-F-RNAi x WT Rab11 overexpression line
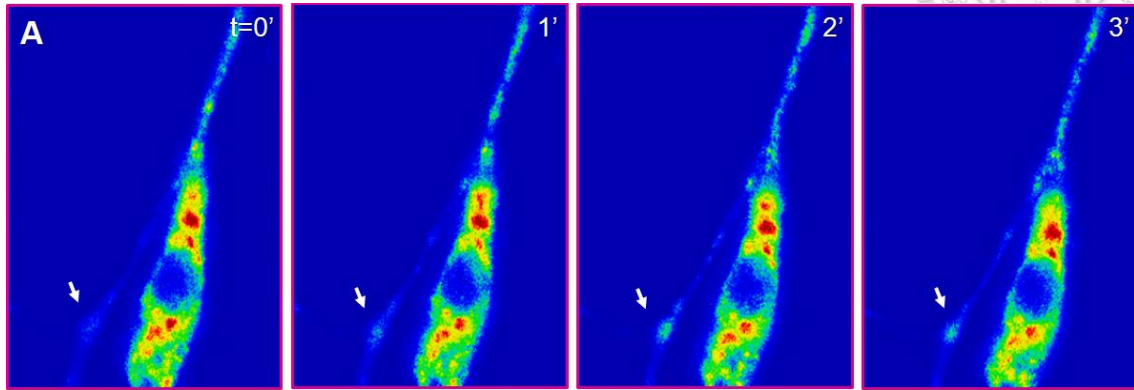
IK2-RNAi x WT Rab11 overexpression line
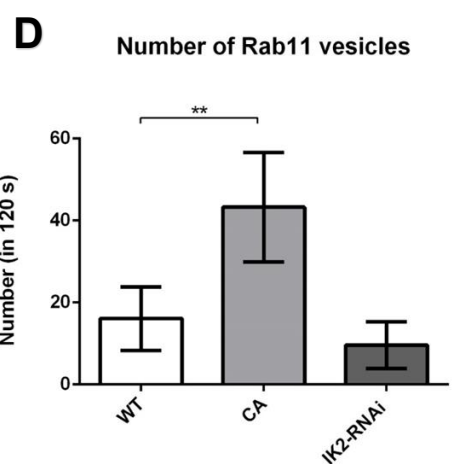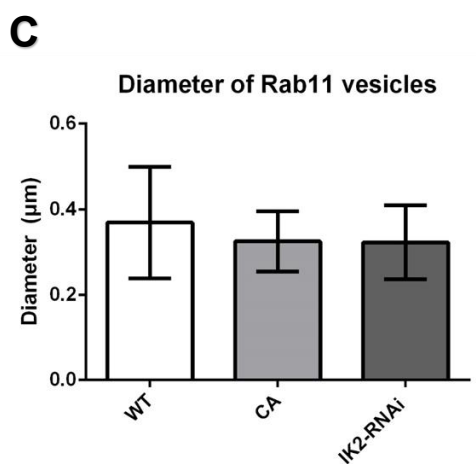

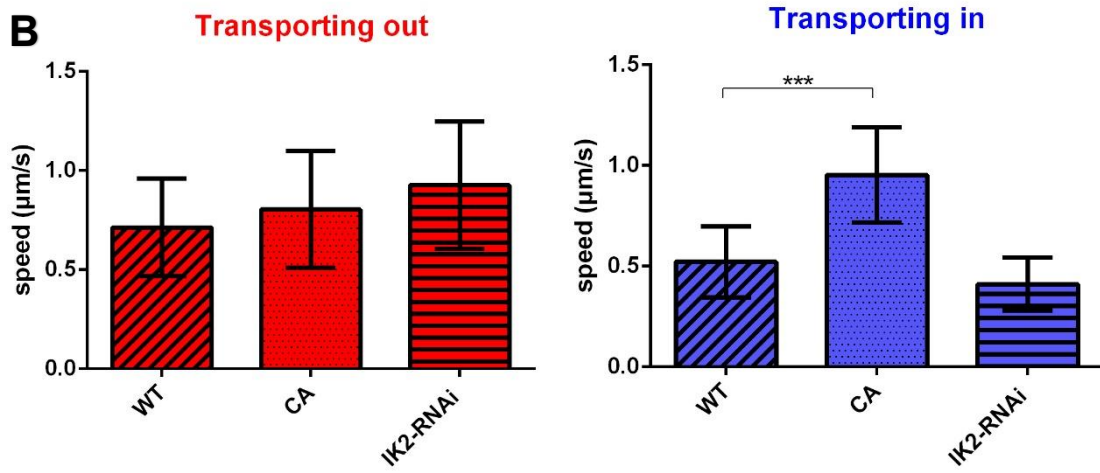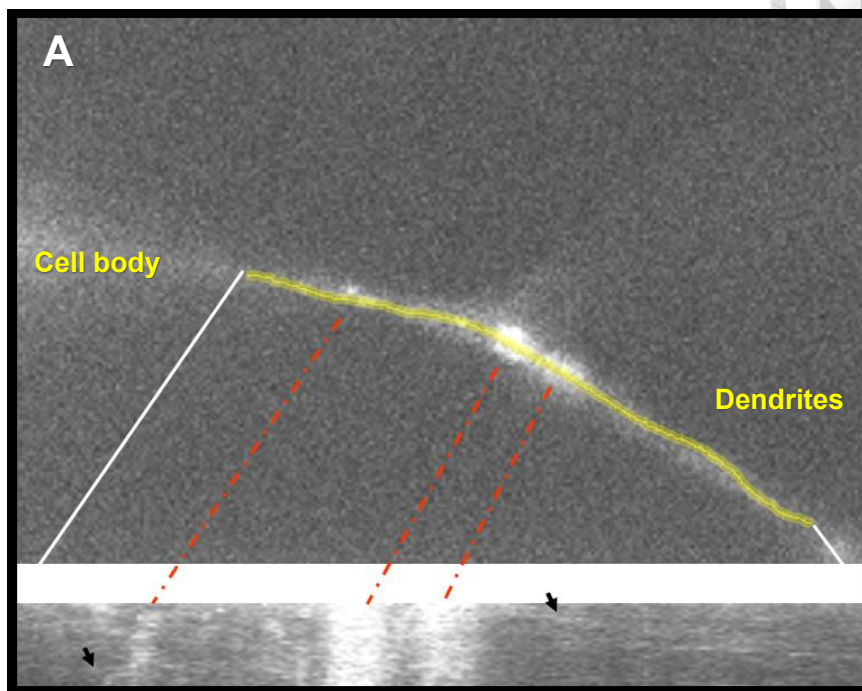**Dhc-RNAi x WT Rab11 overexpression line**

43

Figure 8. Early APF movement of Rab11 in Spn-F, IK2, Dynein heavy chain knock

   out condition.

(A-C) Signals of WT-Rab11in Spn-F, IK2, Dynein heavy chain knock out neurons at early

APF (1-2 hrs APF). Rab11 showed movement on dendrites and variety at branches. The

neuron was visualized with ppk-Gal4,UAS-mCD8-RFP. WT-Rab11-GFP signals were

classified in rainbow color by Zen 2009 software. (A) Nig-Fly 12114-R4 Spn-F-RNAi

(III) (B) UAS-DmIKK(IR)/CyoWeep,Kr>GFP (C) VDRC-28054 Dhc64C-RNAi. The

scale bar represents 10μm.
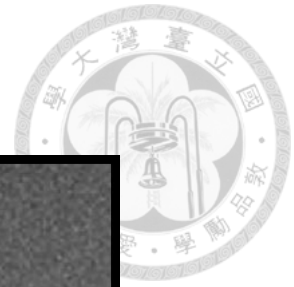
Figure 9

Figure 9. Analysis of Rab11-dependent vesicles in WT, CA-Rab11 overexpression

and IK2 knock down condition.

(A) Kymograph of ppk>WT-Rab11$^{3-1}$-GFP ddaC neuron at early APF, which processed from 30 second time series imagine (interval= 1 second). Rab11 signals were processed with white color. The movement of Rab11 signals had two directions. (B) Analysis of Rab11-dependent vesicle speed. Vesicles were separated into two groups which depended on their direction. (C) Quantification of diameter of Rab11-dependent vesicles. (D) Number of Rab11-dependent vesicles appeared in 2 minutes.

Figure 10

A
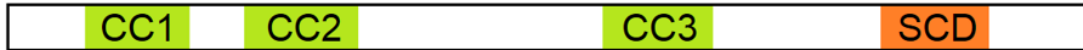
B
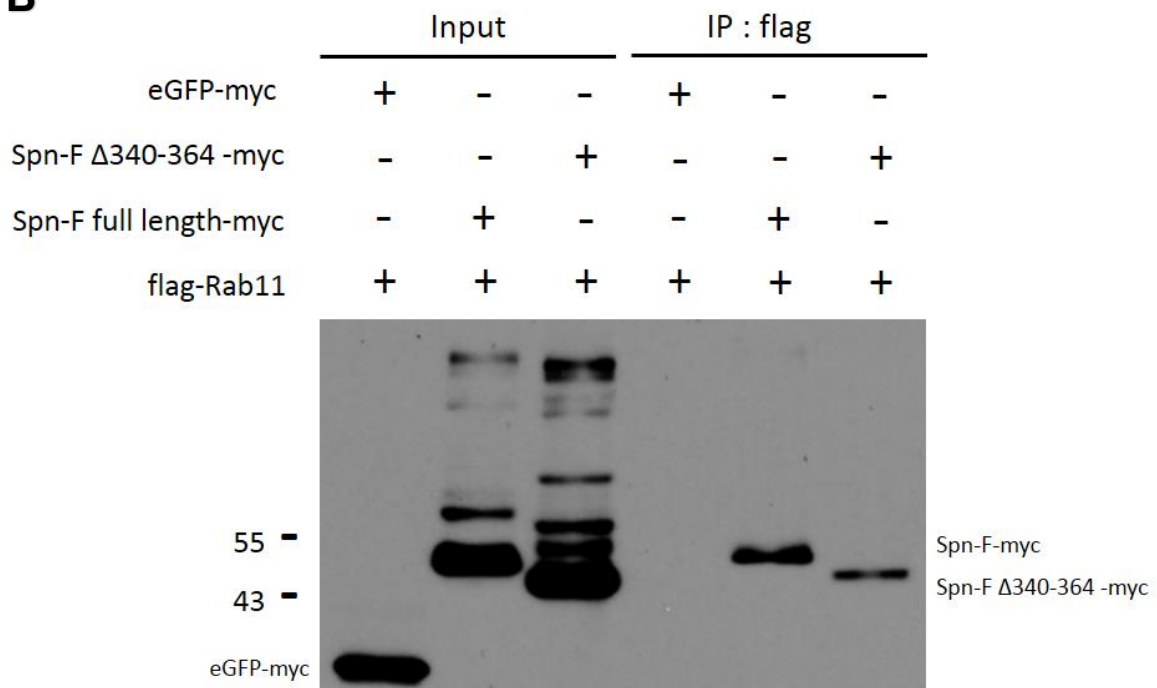
Figure 10. Diagrams of Spn-F△340-364 construct and its association with Rab11

was disturbed compared to full-length Spn-F.

(A) The protein domains of Spn-F which contains three coil-coiled (CC) domains and a

Spn-F conserved domain (SCD). (B) Co-immunoprecipitation of Flag-Rab11 and full

length Spn-F and truncated Spn-F. eGPF-myc as a negative control.

47
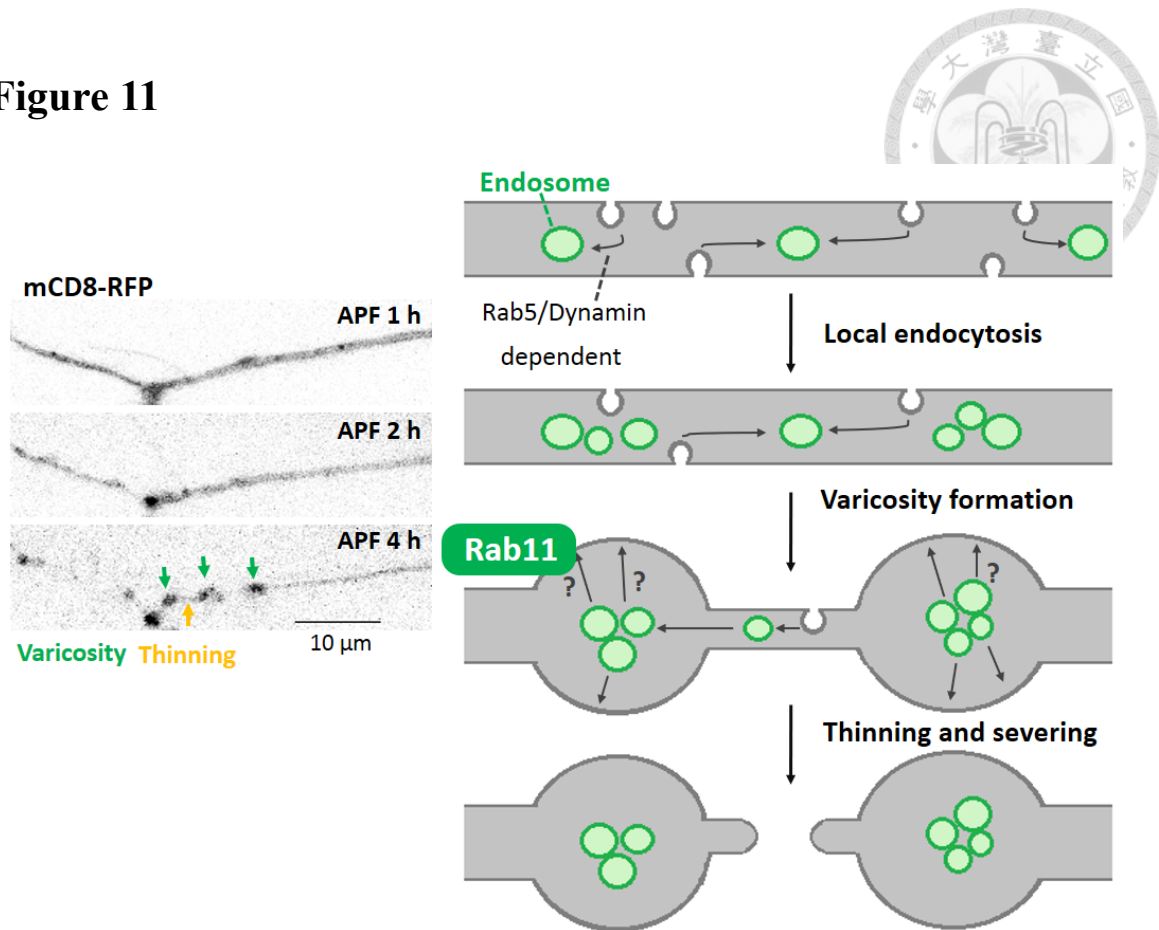
Figure 11

Figure 11. The model of varicosity formation and the possible role of Rab11.

The processed confocal imagines which taken at APF 1,2 and 4 hrs. The dendrites were visualized with p*pk-Gal4,UAS-mCD8-RFP*. RFP signals were processed by Zen 2009 software. Varicosity formation and thinning were observed on dendrite at APF 4 hrs. The scale bar represents 10μm.

Table

Table 1. WT-, CA- and DN-Rab11 sequence

^{1}MGAREDEYDY LFKVVLIGDS GVGKSNLLSR FTRNEFNLES KSTIGVEFAT

^{51}RSIEVDGKTI KAQIWDTAGQ ERYRAITSAY YRGAVGALLV YDIAKHLTYE

^{101}NVERWLRELR DHADQNIVI LVGNKSDLRH LRSVPTDEAK LFAERNGLSF

^{151}IETSALDSTN VETAFQNILT EIYRIVSQKQ IRDPPEGDVI RPSNVEPIDV

^{201}KPTVTADVRK QCCQ

Table 1A. The WT-Rab11 amino acid sequence

	25		70	
Rab11-WT	^{21}GVGK S NLLSR^{30} ----------	^{61}KAQIWDTAG Q ERYRAITSAY^{80}		
Rab11-CA (Q70L)	^{21}GVGK S NLLSR^{30} ----------	^{61}KAQIWDTAG L ERYRAITSAY^{80}		
Rab11-DN (S25N)	^{21}GVGK N NLLSR^{30} ----------	^{61}KAQIWDTAG Q ERYRAITSAY^{80}		

Table 1B. Alignment of CA-, DN-Rab11 amino acid sequences

49

Table 2. The morphology defect of Rab11 mutant fly lines in third larva neurons

Expression level	Rab11 fly lines	Dendritic field reduction	number of total neurons	insertion site
—	W1118	0%	100	—
Medium	CA-8-1	11%	100	III chromosome
Weak	CA-13-19	8%	99	III chromosome
Medium	DN-3-4	100%	100	II chromosome
Medium	DN-8-1 (male)	100%	100	X chromosome
Medium	DN-8-1 (female)	100%	100	X chromosome
Weak	DN-13-2	100%	99	II chromosome

Table 2. The Rab11 mutant fly lines which crossed with p pk-Gal4,UAS-mCD8-GFP (chromosome II)
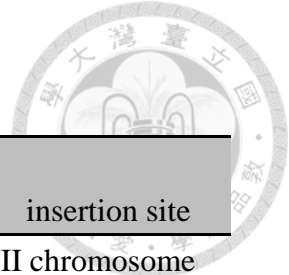
Table 3. The pruning defect of Rab11 mutant fly lines in APF 16 pupa

Expression level	Rab11 fly lines	pruning defect (un-severed)	number of total neurons	insertion site
Strong	CA-16-4	15.91%	88	III chromosome
Strong	CA-16-5	6.41%	78	III chromosome
Medium	CA-8-1	6.67%	90	III chromosome
Weak	CA-13-19	2.86%	70	III chromosome
Strong	DN-5-2	24.49%	98	III chromosome
Strong	DN-19-1	19.80%	101	III chromosome
Medium	DN-6-3 (male)	58.00%	50	X chromosome
Medium	DN-6-3 (female)	37.68%	69	X chromosome
Medium	DN-8-1 (male)	22.22%	81	X chromosome
Medium	DN-8-1 (female)	12.12%	99	X chromosome
Medium	DN-3-4	23.42%	111	II chromosome
Weak	DN-13-2	14.29%	98	II chromosome

Table 3A. The Rab11 mutant fly lines which crossed with ppk-Gal4,UAS-mCD8-GFP (chromosome II)

Expression level	Rab11 fly lines	pruning defect (un-severed)	number of total neurons	insertion site
Strong	CA-16-4	1.25%	80	III chromosome
Strong	CA-16-5	0.00%	50	III chromosome
Medium	CA-8-1	2.50%	80	III chromosome
Medium	CA-8-4	0.00%	90	II chromosome
Weak	CA-13-19	2.00%	50	III chromosome
Strong	DN-5-2	2.50%	80	III chromosome
Strong	DN-19-1	5.00%	100	III chromosome
Medium	DN-3-4	20.49%	122	II chromosome
Weak	DN-13-2	0.00%	49	II chromosome

Table 3B. The Rab11 mutant fly lines which crossed with ppk-Gal4,UAS-mCD8-GFP (chromosome III)

Expression level	Rab11 fly lines	pruning defect (un-severed)	number of total neurons	insertion site
—	W1118	0.00%	60	—
Medium	DN-3-4	0.00%	60	II chromosome

Table 3C. The Rab11 mutant fly lines which crossed with ppk-eGFP (chromosome III)

52